Journal of Alloys and Compounds 471 (2009) 119–121

Contents lists available at ScienceDirect

Journal of Alloys and Compounds

journal homepage: www.elsevier.com/locate/jallcom

Isothermal section of the phase diagram of the ternary system Y–Ni–V at 773 K

Shunkang Pan, Huaiying Zhou *, Qin Zhou, Qingrong Yao, Zhongmin Wang

Department of Information Materials Science and Engineering, Guilin University of Electronic Technology, Guangxi 541004, PR China

ARTICLE INFO

Article history:
Received 26 January 2008
Received in revised form 1 April 2008
Accepted 2 April 2008
Available online 30 June 2008

Keywords:
Rare earth alloys and compounds
Phase diagram
Crystal structure
X-ray diffraction

ABSTRACT

The isothermal section of the phase diagram of the ternary system Y–Ni–V at 773 K was investigated by X-ray diffraction (XRD), scanning electron microscopy (SEM) and energy dispersion spectroscopy (EDS) techniques. It consists of 16 single-phase regions, 29 two-phase regions and 14 three-phase regions. At 773 K, the maximum solid solubility of V in Ni, Y_2Ni_{17}, YNi_5, Y_2Ni_7, YNi_3, and YNi_2, is about 17, 1, 2, 2, 2 and 2 at.%, while Y in Ni, Ni_3V, Ni_2V, Ni_2V_3, NiV_3 and V does not exceed 1 at.%. No ternary compound has been observed in this work.

1. Introduction

Hydrogen storage alloys have attracted considerable attention in view of its potential as an energy storage material. Among them, vanadium and V-based alloys with body-centered cubic (BCC) structure are promising as negative electrode materials for nickel–metal hydride batteries and hydrogen reservoirs for fuel cells, because of their large hydrogen storage capacity per volume, strong resistance to pulverization during hydriding–dehydriding cycles, high-rate of diffusion and rapid activation [1–4]. However, vanadium and V-based alloys are not commercially used because of having poor electro-catalytic activity.

The phase diagrams and thermodynamics are an important basis for the study of the phase transformation of the materials performance. This paper presents the 773 K isothermal section of the Y–Ni–V ternary system phase diagram. The binary subsystems of Y–Ni, Ni–V and Y–V have been widely investigated [5–10]. The crystal structure data on Y–Ni and Ni–V binary compounds are presented in Table 1. The Y–Ni phase diagram was reported in Refs. [5,9,10]. There are nine intermetallic compounds in the Y–Ni system, namely: Y_2Ni_{17}, YNi_5, YNi_4, Y_2Ni_7, YNi_3, YNi_2, YNi, Y_2Ni_2 and Y_3Ni. The V–Ni binary system is taken from Refs. [6,8], and exists in four intermetallic compounds, namely: Ni_3V, Ni_2V, Ni_2V_3 and NiV_3. Ref. [7] reported the Y–V binary phase diagram and no binary compound was observed. Up to now, the phase diagram of the Y–Ni–V ternary system has not been reported.

* Corresponding author.
E-mail address: zhy@guet.edu.cn (H. Zhou).

0925-8388/$ – see front matter © 2008 Published by Elsevier B.V.
doi:10.1016/j.jallcom.2008.04.002

2. Experimental

One hundred and twenty five samples were prepared. Each sample weighs 3 g. The purities of yttrium, nickel, and vanadium used in this work were 99.9%, 99.95%, and 99.9%, respectively. All samples were prepared by melting in an induction furnace under high purity argon. Then, all alloys were sealed in evacuated quartz tubes and put into an automatic controlled resistance heated furnace for homogenization annealing. The heat treatment temperature was determined by the data based on the previous work of Y–Ni and Ni–V binary systems. Some of the samples were homogenized at 1125 K for 18 days and then cooled to 773 K for 12 days. The others were kept at 773 K for a month. Finally, all alloys were quenched into an ice–water mixture.

The samples were powdered and investigated by X-ray diffraction which was carried out on a Rigaku D/Max 2500PC X-ray diffractometer using JADE5 software [11]. The diffraction angles ranged from $2\theta = 20^{\circ}$ to 70° at a voltage of 40 kV and a current of 250 mA. Some samples metallo graphy were analyzed by an S-570 scanning electron microscope (SEM) or by differential thermal analysis (DTA). From all these results, the phase relations in the Y–Ni–V ternary system were determined.

3. Results and discussion

3.1. Binary system

From the analysis of the X-ray diffraction (XRD) patterns of the samples in the Y–Ni–V ternary system in our work at 773 K, we have confirmed the existence of 13 binary compounds in our work. In the Y–Ni system, there are nine binary compounds: Y_2Ni_{17}, YNi_5, YNi_4, Y_2Ni_7, YNi_3, YNi_2, YNi, Y_3Ni_2 and Y_3Ni at 773 K. In the Y–Ni system, there are four binary compounds: Ni_3V, Ni_2V, Ni_2V_3 and NiV_3 at 773 K. No binary compound was found in the Y–V system at 773 K in our work. All the results obtained concerning phase existence and compositions are in perfect agreement with the binary phase diagram reported by Refs. [5–7].

Table 1
The data on the crystal structures of the compounds of the Y–Ni–V system

Phase	Structure type	Space group	Lattice parameters (nm)			Reference
			a	*b*	*c*	
Ni_3V	Al_3Ti	*I4/mmm*	0.35424	–	0.72131	[6,8]
Ni_2V	$MoPt_2$	*Immm*	0.2559	0.7641	0.3549	[6,8]
Ni_2V_3	σCrFe	$P4_2/mnm$	8.966	–	4.641	[6,8]
NiV_3	Cr_3Si	$Pm\bar{3}n$	0.4710	–	–	[6,8]
Y_2Ni_{17}	Th_2Ni_{17}	$P6_3/mmc$	0.8314	–	0.8042	[9,10]
YNi_5	$CaCu_5$	*P6/mmm*	0.4883(1)	–	0.3967(1)	[9,10]
YNi_4	–	–	0.4898	–	4.993	[9,10]
Y_2Ni_7	Ce_2Ni_7	$P6_3/mmc$	0.4928(5)	–	2.411(1)	[9,10]
YNi_3	Be_3Nb	$R\bar{3}m$	0.49779(4)	–	2.449(3)	[9,10]
YNi_2	Cu_2Mg	$Fd\bar{3}m$	0.7181(1)	–	–	[9,10]
YNi	FeB	*Pnma*	0.7156(3)	0.4124(1)	0.5515(2)	[9,10]
Y_3Ni_2	Ni_2Y_3	$P4_12_12$	0.7104	–	3.6597	[9,10]
Y_3Ni	CFe_3	*Pnma*	0.692	0.949	0.636	[9,10]

3.2. *Solid solubility*

The solid solubilities were determined by means of X-ray diffraction (XRD), scanning electron microscopy (SEM) and energy dispersion spectroscopy (EDS) techniques. At 773 K, we have observed that the maximum solid solubility of V in Ni, Y_2Ni_{17}, YNi_5, Y_2Ni_7, YNi_3, and YNi_2, is about 17, 1, 2, 2, 2 and 2 at.%, respectively. The maximum solid solubility of Y in Ni, Ni_3V, Ni_2V, Ni_2V_3, NiV_3 and V as observed does not exceed 1 at.% Y.

3.3. *Isothermal section (773 K)*

By comparing and analyzing the XRD patterns of 125 samples and by identifying the phases in each sample, the isothermal section of the phase diagram of Y–Ni–V ternary system at 773 K was determined, as shown in Fig. 1. The three-phase region $Ni_2Y + NiY + Ni_2V_3$ is (no. 9) of particular interest. The XRD pattern of the alloy $Y_{23}Ni_{50}V_{27}$ which falls in this region and corresponding three-phase equilibrium is illustrated by means of Fig. 2. It consists of 16 single-phase regions, 29 two-phase regions, and 14 three-phase regions. No ternary compound was observed in the 773 K isothermal section.

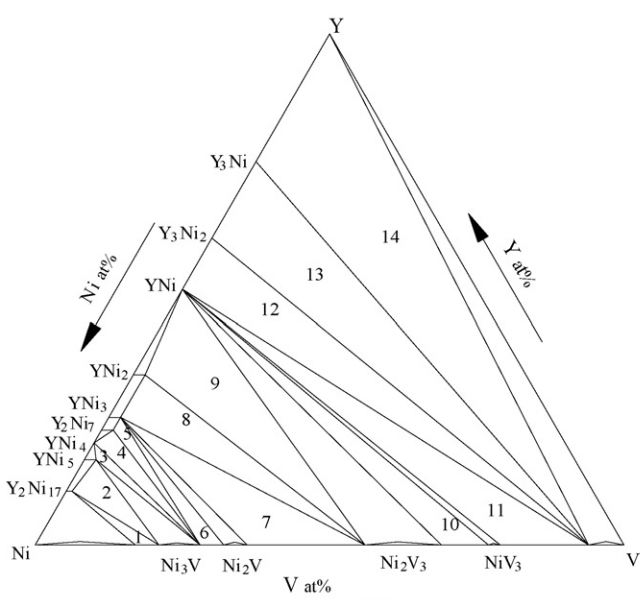

Fig. 1. The 773 K isothermal section of the Y–Ni–V ternary system phase diagram.

Table 2
Three-phase regions and phase relation in Y–Ni–V ternary system at 773 K

Phase region	Phase composition
1	$Ni + Y_2Ni_{17} + Ni_3V$
2	$Y_2Ni_{17} + YNi_5 + Ni_3V$
3	$YNi_5 + YNi_4 + Ni_3V$
4	$YNi_4 + Y_2Ni_7 + Ni_3V$
5	$Y_2Ni_7 + YNi_3 + Ni_3V$
6	$YNi_3 + Ni_3V + Ni_2V$
7	$YNi_3 + Ni_2V + Ni_2V_3$
8	$YNi_3 + YNi_2 + Ni_2V_3$
9	$YNi_2 + YNi + Ni_2V_3$
10	$YNi + Ni_2V_3 + NiV_3$
11	$YNi + NiV_3 + V$
12	$YNi + Y_3Ni_2 + V$
13	$Y_3Ni_2 + Y_3Ni + V$
14	$Y_3Ni + Y + V$

The 16 single-phase regions are: α (Ni), β (Ni_3V), γ (Ni_2V), δ (Ni_2V_3), ε (NiV_3), ζ (V), η (Y), θ (Y_3Ni), ι (Y_3Ni_2), κ (YNi), λ (YNi_2), μ (YNi_3), ν (Y_2Ni_7), ξ (YNi_4), ψ (YNi_5), ω (Y_2Ni_{17}). The 29 two-phase regions are: $\alpha+\beta$, $\beta+\gamma$, $\gamma+\delta$, $\delta+\varepsilon$, $\varepsilon+\zeta$, $\zeta+\eta$, $\eta+\theta$, $\theta+\iota$, $\iota+\kappa$, $\kappa+\lambda$, $\lambda+\mu$, $\mu+\nu$, $\nu+\xi$, $\xi+\psi$, $\psi+\omega$, $\alpha+\omega$, $\beta+\omega$, $\beta+\psi$, $\beta+\xi$, $\beta+\nu$, $\beta+\mu$, $\gamma+\mu$, $\delta+\mu$, $\delta+\lambda$, $\delta+\kappa$, $\varepsilon+\kappa$, $\zeta+\kappa$, $\zeta+\iota$, $\zeta+\theta$. The 14 three-phase regions are: $\alpha+\beta+\omega$, $\beta+\omega+\psi$, $\beta+\psi+\xi$, $\beta+\xi+\nu$, $\beta+\nu+\mu$, $\beta+\gamma+\mu$, $\gamma+\mu+\delta$, $\delta+\mu+\lambda$, $\delta+\lambda+\kappa$, $\delta+\kappa+\varepsilon$, $\varepsilon+\kappa+\zeta$,

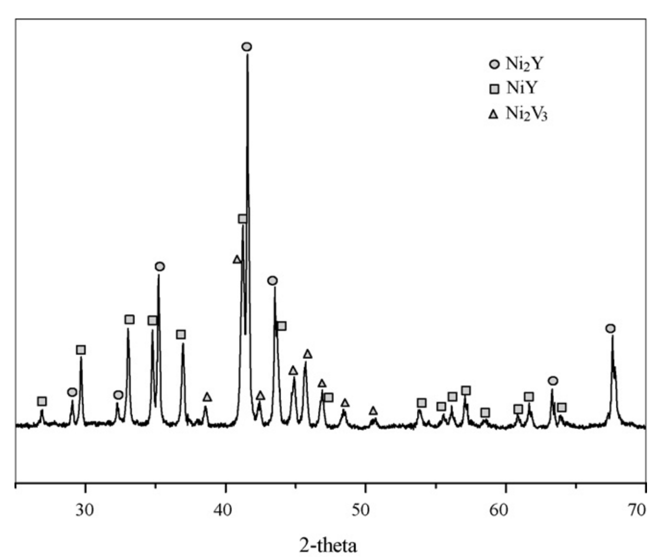

Fig. 2. X-ray diffraction (XRD) pattern of alloy ($Y_{23}Ni_{50}V_{27}$) situated in the three-phase region no. 9.

$\zeta+\kappa+\iota$, $\zeta+\iota+\theta$, $\zeta+\theta+\eta$. Details of the 14 three-phase regions are given in Table 2.

Acknowledgements

This work was supported by the National Natural Science Foundation of China (authorized number: 50571030) and Guilin University of Electronic Technology Natural Science Foundation (project no. YZCL05).

References

[1] A.J. Mealand, G.G. Libowitz, J.F. Lynch, G. Rak, J. Less-Common Met. 104 (1984) 133.
[2] G.G. Libowitz, A.J. Mealand, Mater. Forum 31 (1988) 177.
[3] C.Y. Seo, J.H. Kim, P.S. Lee, J.Y. Lee, J. Alloys Compd. 348 (2003) 252–257.
[4] M.V. Lototsky, V.A. Yartys, I.Y. Zavaliy, J. Alloys Compd. 404–406 (2005) 421–426.
[5] P. Nash, Binary Alloy Phase Diagrams, ASM International, Materials Park, OH, 1991, pp. 2284–2285.
[6] J.F. Smith, O.N. Carlson, P.G. Nash, Binary Alloy Phase Diagrams, ASM International, Materials Park, OH, 1991, pp. 2280–2281.
[7] J.F. Smith, Phase Diagrams of Binary Vanadium Alloys, ASM International, Metals Park, OH, 1989, pp. 318–320.
[8] P. Villars, Pearson's Handbook, Desk ed., pp. 2561–2562.
[9] P. Villars, A. Prince, H.O. Kamoto, Handbook of Ternary Alloy Phase Diagrams, 1995, pp. 1546–1548.
[10] J.F. Smith, Phase Diagrams of Binary Vanadium Alloys, ASM International, Metals Park, OH, 1989, pp. 374–378.
[11] Jade5.0, XRD Pattern Processing Materials Data Inc., 1999.